Developing Electrically Conductive Polypropylene/Polyamide6/Carbon Black Composites with Microfibrillar Morphology

Hamid Garmabi, Sina Naficy*

Department of Polymer Engineering, AmirKabir University of Technology, Tehran, Iran

Received 5 February 2006; accepted 16 May 2007
DOI 10.1002/app.26835
Published online 22 August 2007 in Wiley InterScience (www.interscience.wiley.com).

ABSTRACT: We have established that the PP/PA6/CB composite with 3D microfibrillar conducting network can be prepared *in situ* using melt spinning process. CB particles preferably were localized at the interface between polypropylene as the matrix and PA6 microfibrils, which act as the conducting paths inside the matrix. The percolation threshold of the system reduced when aspect ratio of the conducting phase was increased by developing microfibrillar morphology. The effect of annealing process on the conductivity of PP/PA6/CB composite with co-continuous and microfibrillar morphologies was studied. It was observed that, annealing process forces CB particles towards the interface (2D space) of PP and PA6 co-continuous phases, and percolation threshold and critical exponent of classical percolation theory will be decreased, while the conductivity of conducting composite with microfibrillar morphology was not affected considerably by annealing process at temperatures either higher or lower than the melting point of the PA6 microfibrils. © 2007 Wiley Periodicals, Inc. J Appl Polym Sci 106: 3461–3467, 2007

Key words: carbon black; microfibrillar; morphology; polyamides; polypropylene

INTRODUCTION

Conductive polymer composites (CPCs) are undertaking an important role in technological applications and constitute an ongoing topic of vast commercial interests. These multifunctional materials are routinely employed in various commercial applications due to their good electrical conductivity, corrosion resistance, light weight, and improved mechanical properties.[1]

It is well-known that a polymer composite consisting of an insulating polymeric matrix and conductive fillers becomes electrically conductive as the filler content exceeds a certain critical value, named percolation threshold. This transition-like change in conductivity is generally attributed to percolation phenomena.[2] This transition occurs in percolation threshold concentration of fillers in polymeric matrix.

As a practical point of view, a crucial aspect of the fabrication of the filled conductive polymeric composites is the conducting filler content, which must be as low as possible and still allows the composite to fulfill the electrical requirements. Thus far, several processing techniques have been introduced to lower the conducting percolation threshold in an insulating polymeric matrix.[3–7]

Ongoing attempts to localize conducting particles at the interface or within the minor phase of an immiscible polymer blend have demonstrated that the percolation threshold can be substantially reduced in this manner.[3,5,6] However, two requirements must be fulfilled for the polymer blend composite to be conductive at a lower content of CB. One of these requirements concerns the phase morphology of polymer blend, and another has to do with the heterogeneous distribution of the filler within the polymer blend.

It has been established that the filler geometry influences the phase continuity and selective location of fillers in polymer blend matrices.[8–10] By increasing the aspect ratio of the fillers in the matrix, the lower percolation threshold will be obtained.[11–13] Therefore, if the conducting filler is preferentially localized within the minor phase or at the interface between two blend components, and the minor phase is oriented or elongated to form long conductive microfibers in the polymer matrix, the prepared microfibrillar composite may exhibit higher electrical conductivity, because of the high aspect ratio of the conducting phase.[14]

On the other hand, tailoring the processing parameters of an immiscible polymer blend to form *in situ* reinforced fibers of minor phase inside polymeric matrix is the preferable way to achieve high mechanical properties.[15,16] The preparation of microfibrillar reinforced composites (MFC) includes three basic

Correspondence to: S. Naficy (sn95@uow.edu.au).
**Present address:* Intelligent Polymer Research Institute, University of Woilongong, NSW, Australia.

Journal of Applied Polymer Science, Vol. 106, 3461–3467 (2007)

steps: (1) melt blending using extrusion compounding of two immiscible polymers having various melting temperatures T_m, (mixing step); (2) cold drawing of extrudate resulting in good orientation of two phases (fibrillization step); (3) thermal treatment at a temperature between the T_m's of the two blend partners (isotropisation step). While during the second step, the two polymers are converted into a highly oriented state, the third step results into melting of the component with lower T_m and formation of an isotropic matrix, reinforced with the microfibrils of the component with higher melting temperature.

In this study, we developed a carbon black loaded CPC with microfibrillar structure. The composite was based on polyamide 6 as the dispersed phase and polypropylene (PP) as the matrix. To develop the microfibrils of PA6 inside the PP matrix, horizontal melt spinning process was employed. As in the case of most of the other polymer blend systems, PP and PA6 are thermodynamically immiscible and technologically incompatible, so PP grafted glycidyl methacrylate (PP-*g*-GMA) was prepared and used as the compatiblizer.

EXPERIMENTAL

Materials

The PP was employed as the matrix resin, which was supplied by Arak Petrochemical Co. of Iran (EPC-40R), with MFI of 7 g/10 min (230°C, load 2.16 Kg). Polyamide 6 (PA6) was used as received from BASF (Ultramide® B3) with melt volume flow rate of 130 cm^3/10 min (275°C, load 5 Kg) and T_m = 220°C (10°C/min). The carbon black (CB), which was used as the conductive filler, was donated by Degussa (Printex® XE2B), with dibutyl phthalate (DBP) adsorption value of 420 cm^2/100 g, BET nitrogen surface area of more than 1000 m^2/g and an original particle diameter of 30 nm. PP grafted glycidyl methacrylate, PP-*g*-GMA, was prepared and used as the compatiblizer[17,18] with MFI of 21 g/10 min and grafting level of 3.15 g of GMA per 100 g of PP.

Processing

The composites were prepared applying the following steps. First, CB was premixed with compatiblizer and PP, using a twin screw extruder (Brabender® DSE 25, d = 25 mm, L/d = 32, screw speed = 25 rpm) at a processing temperature of 220°C. However, due to the viscous heating, the real melt temperature is expected to be higher than 220°C, which guarantees the blending of PP phase with compatiblizer and CB particles properly. In all formulations, compatiblizer was added through melt mixing to PP and CB in the twin screw extruder. Then, the mixture of PP/PP-*g*-GMA/CB, which was prepared in previous step, and PA6 granules was fed to a single screw extruder (Brabender Extrusiograph®, d = 19 mm, L/d = 25) equipped with a conical adaptor attached to spinneret die to obtain well developed microfibrillar morphology.

The temperature profile, starting from the feeding zone to the die, was between 220 and 260°C, and the screw rotating speed was maintained fairly constant at 30 rpm. The applied processing conditions correspond to a draw ratio of about 12 for the take off section. Scheme 1 shows the schematic illustration of the premixing step and spinning process to develop microfibrillar morphology.

METHOD

To measure the electrical resistivity of the microfibrillar structured composites, the extruded bristles were compression molded under a pressure of 300 bar for 10 min at 200°C into 1 × 150 × 150 mm^3 plaques. The molding temperature is far above the melting temperature of the PP matrix while it is just under the experimental melting point of PA6 microfibrils (T_m = 220°C), to prevent the PA6 fibers from melting, which is necessary to maintain microfibrillar morphology. Before measuring the electrical resistivity, all of the samples were annealed for 4 h at 190°C to produce an isotropic matrix and microfibril network (isotropisation step). It should be noted that at the annealing temperature of 190°C, the PP matrix has been melted and forms an isotropic matrix, while the PA6 fibers keep their solid like fibrillar structures.

The electrical resistivity of CB-polymer blends was measured using a four point probe technique so that they were free from resistance of sample-electrode contacts.

A scanning electron microscope (Scanning Micro Analyzer JXA840, JEOL) was used for morphological observations. The specimens were frozen in liquid nitrogen, and then quickly impact fractured. To investigate the morphology of the composites, samples were immersed in hot xylene to etch away the PP

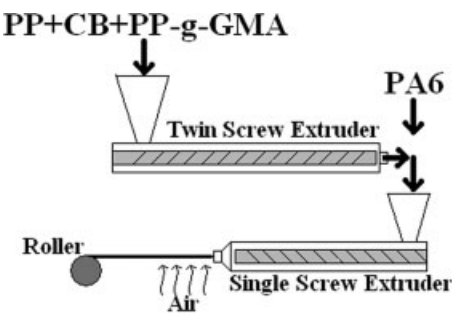

Scheme 1 Schematic illustration of the processing steps.

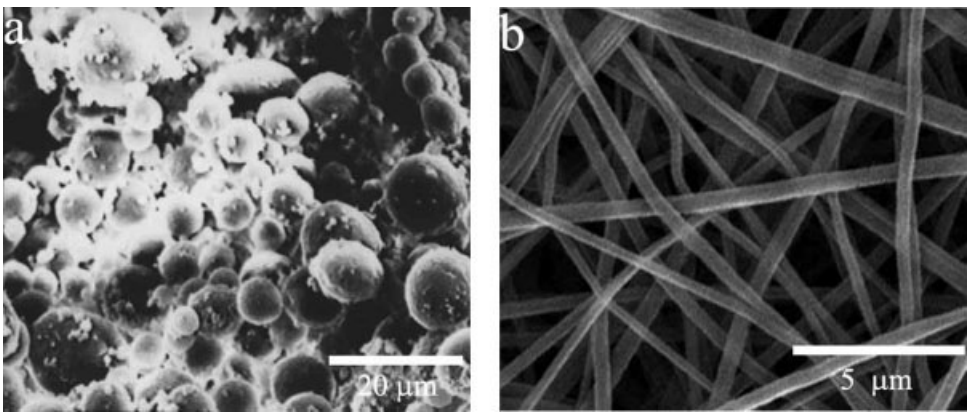

Figure 1 SEM micrograph of freeze-fractured surface of (a) directly mixed PP/PA6 and (b) PP/PA6 microfibrillar composite.

matrix. In some samples PA6-microfibrils were selectively extracted by immersing the samples inside the formic acid for 24 h.

RESULTS AND DISCUSSION

Figure 1(a) illustrates the SEM micrograph of fractured surface of PP/PA6 blend containing 10 wt % of PA6 and compatiblizer content of about 5 wt % before melt spinning process, while PA6 phase was etched away by formic acid. A typical matrix/dispersed morphology with homogeneous dispersion of PA6 droplets in PP matrix is observed, and by a rough estimation the diameter of PA6 droplets is about 12 μm. The SEM microphotograph of the same sample without CB after fiber spinning process is shown in Figure 1(b). It is clear that, during spinning process the blend components are transformed into a highly oriented state. An estimation of the thickest and thinnest PA6-microfibrils leads to values of 1 μm and 500 nm. As presented, the obtained PA6-microfibrils are much longer than the detected zone and the aspect ratio could not be estimated using this micrograph.

Figure 2(a) shows the morphology of the PP/PA6/CB compression molded composite containing 4 wt % of CB, 10 wt % of PA6 and compatiblizer content of 5 wt % after melt spinning process. In this figure, the PP matrix was selectively extracted by hot xylene. Apparently, the well defined PA6 microfibrils rich in CB were generated *in situ*; although according to the processing section, CB particles were initially premixed with PP and compatiblizer using a twin screw extruder. From rough measurements, the average diameter of microfibrils is estimated about 6 μm.

Figure 2(b) presents the SEM micrograph of the same sample while PA6 microfibrils were etched away by formic acid. Taking into account the composition of the ternary composite, it is clear that the continuous phase is PP. The average aspect ratio of the microfibrils, in visible region, is about 19; however, higher aspect ratios could be obtained in low magnification micrographs.

There has been a long history of investigation of fibrillation of the dispersed phase inside a matrix, in

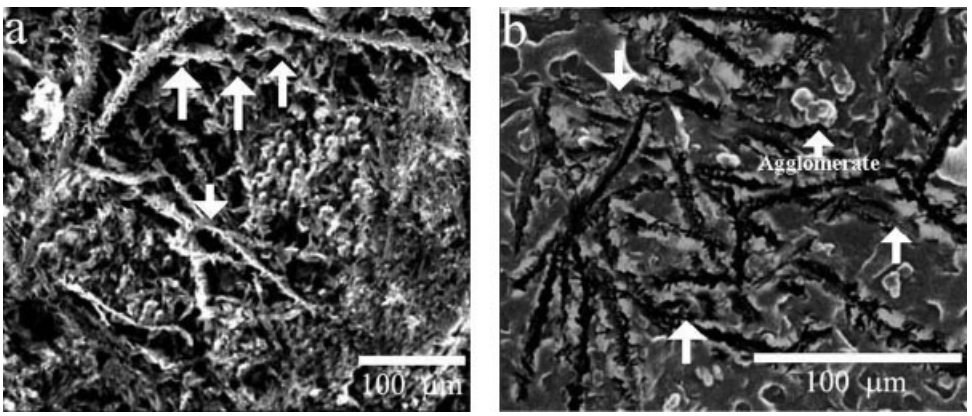

Figure 2 SEM micrograph of the PP/PA6/CB composite; (a) PP matrix was etched away by hot xylene, (b) PA6-microfibrils was selectively extracted by formic acid. The arrows indicate the CB particles.

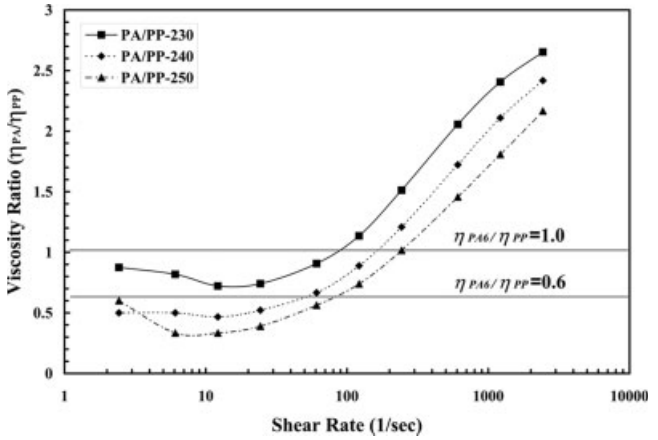

Figure 3 Viscosity ratio (PA6/PP) as a function of shear rate at 230, 240, and 250°C.

an incompatible polymer blend. With the aid of morphological and rheological studies, the mechanism of deformation of the dispersed droplets during melt processing of incompatible polymer blends was declared.[19–21] Many studies have shown that elongational flow field incorporated with small viscosity ratio of the dispersed phase to matrix[22] ($\eta_d/\eta_m \approx 0.6$) can facilitate fibrillation of the dispersed phase. To fulfill the appropriate viscosity ratio, the PP and PA6 resins were selected through rheological studies using a capillary rheometer (Rheoscop 1000, Ceast). Figure 3 shows the viscosity ratio of PA6/PP at 230, 240, and 250°C. The rheological studies approved that the viscosity ratio (η_{PA6}/η_{PP}) was lower than unity up to the shear rates of about 200 s^{-1} at the temperature of 250°C. When the CB was compounded into the polymer blend, the melt viscosity of the system increased noticeably. As illustrated in Figure 2, because of the presence of CB particles at the interface of PP and PA6 phases and also inside the PA6 phase, the effective viscosity ratio increases which inhibits large deformations of PA6 droplets and accordingly the fibrillation capacity of the PA6-containned CB interface was reduced considerably. As a result, the diameter of the PA6 microfibrils incorporating CB either at the interface or within the PA6 microfibrils [Fig. 2(b)] was roughly measured 6 μm, while the diameter of the microfibrils in the system without CB was estimated about 0.5–1 μm.

Higher affinity of the CB to the PA6 resin compared to the nonpolar resins such as PP has been observed in the previous studies.[23,24] In Figure 2, the small particles with irregular geometry are CB agglomerates. Although the CB particles were added to the PP matrix through twin screw compounding before adding the PA6 resin in fibrillization process, CB particles are mostly accumulated either at the interface or within the PA6 microfibrils (arrows in Fig. 2). Therefore, it can be concluded that the CB particles were preferentially localized either at the interface or within the PA6 microfibrils.

Generally, competitive adsorption of polymer melts on a solid surface is determined by CB-polymer interaction. When CB particles are mixed with a polymer blend consisting of polymer A and B, the location of CB should be predicted by Young's equation[25]

$$y = (\gamma_{CB,A} - \gamma_{CB,B})/\gamma_{A,B} \quad (1)$$

where $\gamma_{CB,A}$, $\gamma_{CB,B}$, and $\gamma_{A,B}$ are interfacial energy between polymer A and CB, between polymer B and CB, and between polymers A and B, respectively. CB particles are expected to be selectively located in one of the two polymer phases where the polymer has a higher interaction with the CB surface: $y > 0$ means $\gamma_{CB,A} > \gamma_{CB,B}$ or CB particles are supposed to be in polymer B, while $y < 0$ means $\gamma_{CB,A} < \gamma_{CB,B}$ or CB particles are preferably located in polymer A. Interfacial energy can be calculated by:[26]

$$\gamma_{1,2} = \left[\left(\gamma_1^d\right)^{1/2} - \left(\gamma_2^d\right)^{1/2}\right] + \left[\left(\gamma_1^p\right)^{1/2} - \left(\gamma_2^p\right)^{1/2}\right] \quad (2)$$

where $\gamma_{1,2}$, γ_1^d (or γ_2^d), and γ_1^p (or γ_2^p) are interfacial energy, dispersive part of interfacial energy and polar part of interfacial energy, respectively, and subscripts 1 and 2 indicate materials 1 and 2 (CB, PP, PA6). According to available literatures[26,27] and Eq. (2), the interfacial energy between CB and PP is calculated 19.8 mJ/m^2, and between CB and PA6 is calculated 17.1 mJ/m^2. As stated before,[23,24] and according to the Young's equation ($\gamma_{CB,PA6} < \gamma_{CB,PP}$), a high probability exists that CB is better adsorbed to PA6 than to PP because of a lower interfacial energy between PA6 and CB in comparison to PP and CB, or a larger compatibility between CB and PA6.

Electrical conductivity has systematically been measured for compression molded samples. Electrical conductivity of the prepared samples σ as a function of CB content is shown in Figure 4 which presents a typical percolation behavior. In ''classical'' percolation theory, continuity of second phase's pathway yields the typical power-law dependence of electrical conductivity σ on the weight fraction (or volume fraction) of the conducting phase w:

$$\sigma \approx \sigma_f (w - w_c)^t \quad (3)$$

where t is critical exponent and σ_f is final conductivity of composite, which will be achieved when $w \rightarrow 1$. w_c is percolation threshold of the system, where the conductivity of the composite jumps from insulating zone to the conducting zone. At this concentration the content of conducting fillers (CB particles) is enough to form conductivity pathways.

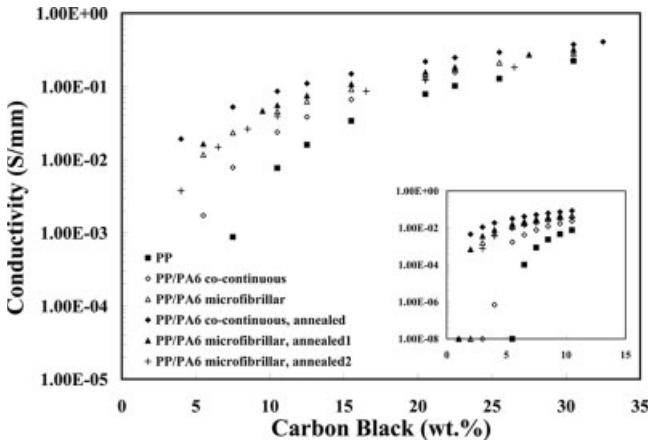

Figure 4 Conductivity versus CB content. (■) semicrystalline PP matrix (220°C, 10 min). (◇) co-continuous PP/PA6 (55:45) blend (250°C, 10 min). (Δ) microfibrillar PP/PA6 (80:20) blend (200°C, 10 min). (◆) co-continuous PP/PA6 (55:45) blend annealed at 250°C, 120 min (▲) PP/PA6/CB microfibrillar composite annealed at 200°C, 120 min, (annealed1). (+) PP/PA6/CB microfibrillar composite annealed at 250°C for 120 min (annealed2). The inset magnifies the conductivity of composites for the sake of clarity.

For the specimens of this work, the concentration of the conductive filler is expressed in per cent weight of the conductive particles. Equation (3) can be rewritten adding a new coefficient c,

$$\sigma = \sigma_f (w - w_c)^t + C \quad (4)$$

This coefficient c represents the conductivity of the specimen when the concentration is equal to the critical concentration ($w \sim w_c$, $c \sim \sigma_c$). The value of the four parameters w_c, t, c, and σ_f was derived by fitting eq. (4) to the experimental data. The aim of this method is to relate all four parameters so that if w_c is found then the others can be calculated. The method follows four steps as follows. At the first step, from the plot of conductivity–concentration, the experimental points that clearly show an abrupt increase in conductivity are taken into consideration. For these experimental points, a regression is performed using the equation $\sigma = Aw^b$, and by least square method coefficients A and b are determined. Then a value for w_c is estimated from the plot of conductivity–concentration, and c is computed from $c = \sigma_c = A(w_c)^b$. In the next step, eq. (4) is considered to be equal to $\sigma = Aw^b$ for concentration $w = 1 + w_{c,}$ in order to correlate the coefficient σ_f with A, b, and $w_{c,}$ while t is eliminated. Thus the following relation is obtained,

$$\sigma_f = A\left[(1 + w_c)^b + (w_c)^b\right] \quad (5)$$

When σ_f was calculated from Eq. (5), a value for t is obtained from Eq. (4) with the use of just one experimental point. All the above evaluations of the unknown parameters are not the correct ones. They are the first estimations of these parameters. To correct these estimations, equations (4) and $\sigma = Aw^b$ are compared in a space near the percolation threshold. The comparison of the two equations is achieved by computing the definite integral of their absolute difference Δw_c). The integral is considered to be a function of the percolation threshold w_c,

$$\Delta(w_c) = \int_{w_c}^{w_c + \delta} \left| [\sigma_f (w - w_c)^t + c] - A(w)^b \right| dw \quad (6)$$

The value of δ is obtained such that the above integral becomes minimized, and therefore the corrected value for w_c is consequently obtained. From the corrected value of percolation threshold the other three parameters are evaluated again.[28]

Figure 4 also shows a comparison between a microfibrillar structured PP/PA6/CB composite (PP/PA6: 80/20), and a PP/PA6/CB composite (PP/PA6: 55/45), compression molded at 250°C for 10 min with co-continuous morphology. The compression molding of microfibrillar structured composites was performed at 200°C for 10 min to guarantee the fluidity of PP matrix while the molding temperature was just below the melting temperature of PA6-microfibrils (T_m = 220°C), to prevent from melting of PA6-microfibrils during molding process. In Figure 5, the thermal behavior of samples was examined using a differential scanning calorimeter (DSC). The experiment was done using a heating rate of 10°C/min from 50 to 300°C. The DSC curves of PP, PA6, and PP/PA6/CB blend with various CB compositions are presented in Figure 5, showing distinct

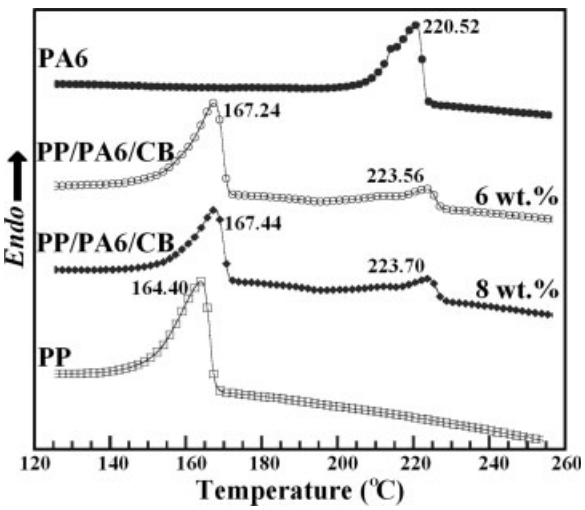

Figure 5 DSC melting curves of PP(□), PA6 (●), PP/PA6 (80 : 20) with 6 wt % of CB (○) and PP/PA6 (80 : 20) with 8 wt % of CB (◆).

melting temperatures as can be seen. According to this figure, the melting point of both two phases increases slightly with increasing CB portion. This may indicate that there is an increase in the number of nuclei[29] in the presence of extraneous particles such as CB.

To study the effect of annealing temperature on the conductivity and structure of both microfibrillar structured and co-continuous composites, annealing process was performed on PP/PA6/CB co-continuous composite at a temperature higher than melting point of PA6 ($T_{\text{anneal.}}$ = 250°C, 120 min). Also annealing process was performed on PP/PA6/CB microfibrillar composites, at temperatures lower ($T_{\text{anneal.,1}}$ = 200°C, 120 min) and higher ($T_{\text{anneal.,2}}$ = 250°C, 120 min) than melting temperature of PA6-microfibrils.

As illustrated by Figure 4, for the PP/PA6/CB composites with co-continuous morphology when $T_{m,\text{PA6}} < T_{\text{anneal.}}$ = 250°C, and also for the microfibrillar morphology when $T_{\text{anneal.,1}}$ = 200°C < $T_{m,\text{PA6}}$, the percolation threshold and critical exponent decreased upon the annealing process.

Table I lists the fitting parameters, w_c and t, for the data presented in Figure 4. According to Table I, t is found to be 1.99 when CB was dispersed within the amorphous phase of pure PP. When CB was dispersed in the PP matrix of a PP/PA6 blend with co-continuous morphology, t decreases to 1.8, and by developing microfibrillar morphology during spinning process, t was reduced further to 1.5.

Indeed, when the CB filled polyblends with dual-phase continuity compression molded at 250°C for 10 min, a percolation threshold of ~ 4 wt % is observed, which is comparable to the value reported for the selective localization of CB (Printex® XE2B) in PE phase of the PE/PS (45/55) blend (~ 3 wt %).[30] Also a lower percolation threshold was achieved for microfibrillar composite (~ 2.1 wt %) than the co-continuous one. However, when the compression molding time of the blend with dual-phase continuity at 250°C was increased up to 120 min during the annealing process, the phase morphology has the opportunity to recognize in such a way that the percolation threshold was decreased down to 1 wt % and the critical exponent t was equal to 1.3, which are the typical values for a 2D system.[31] This effect indicates an increase in the local CB concentration as a result of decreased interfacial area, which is the spontaneous tendency of an immiscible polymer blend in the melt state in absence of shear forces. It is also clear that the CB particles do not leave the interface under conditions of zero shear rate, but rather concentrate more uniformly in this region.

On the other hand, annealing the microfibrillar structured composite at 200°C for 120 min had no significant effect on the critical exponent t, while reduced percolation threshold of the system to ~ 1.5 wt %. This is probably due to the fact that annealing temperature was under the melting point of the PA6-microfibrils and hence enabled the composite to keep its microfibrillar structure. Also, forcing the CB particles to concentrate more uniformly near the interface could be another explanation for the observed reduction of percolation threshold. On the other hand, annealing at a temperature higher than the melting point of the PA6-microfibrils (250°C for 120 min), deteriorates the microfibrillar structure and t decreases to 1.4 while percolation threshold increases to about 2.5 wt % of CB.

TABLE I
Effect of Annealing Process on the Power Law Parameters of CB filled PP and PP/PA6 with Co-continuous and Microfibrillar Morphology

CB dispersed in:	Percolation threshold (wt %)	Critical exponent t
PP matrix	5.98	2.0
PP/PA6 (55 : 45) Co-continuous	3.98	1.8
PP/PA6 (90 : 10) Microfibrillar	2.1	1.5
PP/PA6 (55 : 45), annealed at 250°C Co-continuous	1	1.3
PP/PA6 (90 : 10), annealed at 200°C Microfibrillar	1.51	1.5
PP/PA6 (90 : 10), annealed at 250°C Microfibrillar	2.5	1.4

CONCLUSIONS

In conclusion, we have developed PP/PA6/CB composites with microfibrillar morphology, using melt spinning process. The CB particles were mainly localized at (or near) the interface of the PP and PA6 phases or within the PA6 phase, due to higher interaction of the PA6 with the CB surface. It is totally advantageous to conductivity that the CB particles localized at the interface of microfibrils to act as conducting paths and reducing the percolation threshold more than four times in comparison to PP.

S. Naficy is thankful to Prof. R. Bagheri of the Isfahan University for encouragement and discussions on DSC and some of the electrical experiments.

References

1. Rupprecht, L., Ed. Conductive Polymers and Plastics: In Industrial Applications; William Andrew Inc.: New York, 1999.
2. Zhang, M. Q.; Xu, J. R.; Zenge, H. M.; Yun, F. C.; Zhang, Z. Y.; Friedrich, K. J Mater Sci 1995, 30, 4226.

3. Gubbels, F.; Blacher, S.; Vanlathem, E.; Jerome, R.; Deltour, R.; Brouers, F.; Teyssie, Ph. Macromolecules 1995, 28, 1559.
4. Thongruang, W.; Spontak, R. J.; Balik, C. M. Polymer 2002, 43, 3717.
5. Zhang, M. Q.; Yu, G. Macromolecules 1998, 31, 6724.
6. Calberg, C.; Blacher, S.; Gubbels, F.; Brouers, F.; Deltour, R.; Jerome, R. J Phys D: Appl Phys 1999, 32, 1517.
7. Dong, X. M.; Fu, R. W.; Zhang, M. Q.; Zhang, B.; Li, J. R.; Rong, M. Z. Carbon 2003, 41, 369.
8. Zhang, G. M. Phys Rev B 1996, 53, 6256.
9. Xue, Q. Eur Polym J 2004, 40, 323.
10. Nettelblad, B.; Martensson, E.; Onneby, C.; Gafvert, U.; Gustafsson, A. J Phys D: Appl Phys 2003, 36, 399.
11. Celzard, A.; McRae, E.; Deleuze, C.; Dufort, M. Phys Rev B 1996, 53, 6209.
12. Philipse, A. P. Langmuir 1996, 12, 1127.
13. Saar, O. M.; Manga, M. Phys Rev E 2002, 65, 056131.
14. Li, Z. M.; Xu, X. B.; Lu, A.; Shen, K. Z.; Huang, R.; Yang, M. B. Carbon 2004, 42, 428.
15. Fakirov, S.; Evstatiev, M. Polymer Blends (Volume 2: Performance: Polymer Blends to Microfibrillar Reinforced Composites); Paul, D. R.; Bucknall, C. B., Eds.; Wiley: New York, 2000; p 455.
16. Golmohamadi, S.; Garmabi, H. MSc theses, AmirKabir University of Technology, Tehran, Iran, 2004.
17. Golmohamadi, S.; Garmabi, H. Paper presented at PPS2004, Hanover, Germany, 2004.
18. Friedrich, K.; Evstatiev, M.; Fakirov, S.; Evstatiev, O.; Ishii, M.; Harrass, M. Compo Sci Tech 2005, 65, 107.
19. Salem, D. R., Ed. Structure Formation in Polymeric Fibers; HANSAR: Cincinnati, 2000.
20. Almusallam, A. S.; Larson, R. G.; Solomon, M. G. J Rheol 2000, 44, 1055.
21. Almusallam, A. S.; Larson, R. G.; Solomon, M. G. J Non Newtonian Fluid Mech 2003, 113, 29.
22. Favis, B. D. Polymer Blends (Volume 1: Formulation: Factors influence the morphology of immiscible polymer blends in melt processing); Paul, D. R., Bucknall C. B., Eds.; Wiley: New York, 2000; p 502.
23. Tchoudakov, R.; Breuer, O.; Narkis, M.; Siegmann, A. Polym Eng Sci 1996, 36, 1336.
24. Srivastava, S.; Tchoudakov, R.; Narkis, M. Polym Eng Sci 2000, 40, 1522.
25. Sumita, M.; Sakata, K.; Asai, S.; Miyasaka, K.; Nakagawa, H. Polym Bull 1991, 25, 265.
26. Wu, S. Polymer interface and adhesion; Marcel Dekker: New York, 1982.
27. Wu, G.; Asai, S.; Sumita, M.; Yui, H. Macromolecules 2002, 35, 945.
28. Tsangaris, G. M.; Kazilas, M. C. Mater Sci Tech 2002, 18, 226.
29. del Río, C.; Ojeda, M. C.; Acosta, J. L. Eur Polym J 2000, 36, 1687.
30. Gubbels, F.; Jerome, R.; Vanlathem, E.; Deltour, R.; Blacher, S.; Brouers, F. Chem Mater 1998, 10, 1227.
31. Clerc, J. P.; Giraud, G.; Laugier, J. M.; Luck, J. M. Adv Phys 1999, 39, 191.